Progress In Electromagnetics Research B, Vol. 101, 175–191, 2023

High-Isolation and Side Lobe Level Reduction for Dual-Band Series-Fed Centre-Fed X/Ku Shared Aperture Binomial Array Antenna for Airborne Synthetic Aperture Radar Applications

Praveena Kati and Venkata Kishore Kothapudi*

Abstract—This research paper introduces a novel dual-band single-polarized (DBSP) series-fed center-fed open stub (SFCFOS) Binomial Antenna Array synthesis technique to improve side lobe levels (SLL) and better isolation for the use in Airborne Synthetic Aperture Radars (AIR-SARs). The antenna utilizes a shared-aperture array (SAA) architecture, operating in both X- and Ku-bands with center frequencies of 9.3 and 13.265 GHz with a frequency ratio of 1 : 1.426. The SAA consists of a 7-element linear array of square microstrip patches for the X/Ku-band. The inter-element spacing between patches is set at 0.7λ to meet the $\pm 25^\circ$ scan range requirements. The X-band (9.3 GHz) frequency is ideal for soil moisture estimation in agricultural areas, while the Ku-band (13.265 GHz) is suitable for applications in snow-covered regions, cold areas, and disaster monitoring. To validate the antenna design, a prototype is fabricated and tested for S-parameters, radiation characteristics, and gain measurements. The size of the shared-aperture antenna is 200 mm × 50 mm × 0.787 mm. The measured results of the prototype align well with the simulated ones, exhibiting excellent radiation performance and high isolation. The bandwidth of 1.07% (X-band) and 1.5% (Ku-band) and return loss of 25 dB/−15.7 dB at 9.3/13.265 GHz are achieved. The measured isolation is −45 dB which provides a large signal separation at X/Ku-bands. The antenna design shows a side-lobe level (SLL) of −39.5 dB at E-plane ($\varphi = 0^\circ$ and −17.9 dB for H-plane ($\varphi = 90^\circ$) for the X-band and −35 dB at $\varphi = 0^\circ$ −19 dB for H-plane ($\varphi = 90^\circ$) for the Ku-band. Additionally, it achieves high gain values of 12.8 dBi for the X-band and 13.2 dBi for the Ku-band. This research presents the first reported shared-aperture X/Ku-band single polarized planar array with binomial amplitude distribution synthesis technique, which holds significant value for AIR-SAR applications. All the measured results were in line with simulated ones and matched reasonably well.

1. INTRODUCTION

Synthetic Aperture Radar (SAR) has been widely used for Earth remote sensing for more than 30 years [1, 2]. AIR-SARs are very useful over a wide range of applications, including sea and ice monitoring, mining, oil pollution monitoring, oceanography, snow monitoring, and classification of Earth terrain [3–8]. The Shuttle Imaging Radar (SIR)-C/X SAR (operating with L/C/X-bands of weight around 3000 kg) on the American Space Shuttle Endeavour (ASSE), a high-resolution 3D imaging radar, acquired images for first time throughout the world in 2000 [9]. It consists of three individual dual-polarized sub-arrays. An SAA compact design for L- and C-bands is proposed by Axness et al. [10] to overcome the limitations of SAR antenna designs. More commonly, dual-band antenna design can be achieved by either two single-band elements or one dual-band element or multilayer configuration based on microstrip patch

Received 12 April 2023, Accepted 14 July 2023, Scheduled 28 July 2023
* Corresponding author: Venkata Kishore Kothapudi (v.k.kothapudi@ieee.org).
The authors are with the Center of Excellence Advanced RF Microwave & Wireless Communications, Department of Electronics and Communication Engineering, School of Electrical, Electronics, and Communication Engineering, Vignan's Foundation for Science, Technology, and Research (VFSTR), Vadlamudi, Guntur District, Andhra Pradesh 522213, India.

antenna technology [11]. The use of two single-band elements (either single or multilayer) is always considered to be a more efficient antenna aperture than conventional designs with a high-frequency ratio of more than 2. In [12], a tri-band L/S/X system with a frequency ratio of $1 : 2.8 : 8$ was proposed with a 5-layer configuration. A Bifunctional Metasurface technique with a shared aperture concept was introduced in [13] with an FR of 2.4 at S/C-band having gains of 7.9 dBi and 2.7 dBi. A 2-layer Ku/Ka-band with a frequency ratio of 2.1 by using the Structure-Reuse Technique has been implemented with < 9 dBi gain having an array size of $2 \times 3/4 \times 4$ [14]. A Metamaterial-Based S/X-Band Shared-Aperture Phased-Array Antenna with frequency ratio of $2.7 : 1$ having a multilayer configuration with a gain of 7.6 dBi and scan angle $\pm 50^{\circ}$ is implemented in [15]. An SAA with single and dual polarizations has been implemented with Ku/Ka-band with an isolation of 30 dB [16]. A 2D SAA with Ku- and Ka-band multilayer 8×8 array has been implemented with a gain of 22 dBi at both the bands and an isolation of 30 dB in [17]. An SAA with radiation pattern distortion technique has been implemented with FR of 2.1 and achieved with multilayer configuration with a gain of 7.3/13 dBi at both S/L bands in [18]. A dual-band, dual-circularly-polarized shared-aperture SAA with high highly isolated RF power is used in [19] as an information receiving system. In [20], an SAA with cavity Slot Antenna-in-Package with Enhanced Beam Coverage for MIMO applications has been implemented. In [21], an SAA with dual-band multi-polarization at Ku-/Ka-band for Satellite Communication with a gain of 18 dBi/23.4 dBi and isolation of 15 dB has been implemented. In [22], a K-/Ka-Band Shared-Aperture Phased Array with the gain of 4.5 dBi and isolation of 40 dB was achieved. In [23], a research design operates at L-, S-, and X-bands with an approximate frequency ratio of $1 : 1.9 : 5.5$. Three types of radiation elements resonating at different frequencies, including the square microstrip patch, microstrip dipole, and printed monopole, are interlaced in the same aperture. A simple metallic strip (MS), comprising four metal stubs and one rectangle-shaped metal pillar, is utilized to improve the inter-element isolation of the array in and between the C- and S-bands [24]. A shared aperture multilayer antenna operating at both S- and X-bands for airborne SAR applications was presented in [25]. The authors in [26–29] reported a series of designs with a 10-element uniform linear array, Chebyshev amplitude distribution array, hybrid-fed array (combination of series-fed and corporate-fed), and 1×2, 2×2, and 3×3 series-fed X-band arrays with complete s-parameters and radiation characteristics have been analyzed. In [30], a series-fed binomial array has been implemented with extreme side-lobe levels.

In [31], an investigation has been done with binomial and Chebyshev distribution for linear and rectangular dielectric resonator antenna arrays. In [32], a 23-element series fed linear array at Ka-band gives a gain of 19 dBi with a beam in broadside direction and has SLL better than -15 dB. A 7-element series-fed antenna array yielded a measured gain of 15.1 dBi at 5.79 GHz. In [33], linear arrays along radiating (E-plane) and non-radiating (H-plane) edges are designed for broadside radiation patterns at 5.8 GHz using U-shaped series- and corner-feed configurations, respectively. Ref. [34] describes a power-efficient method of beamforming algorithm by using a novel concept of Fractional-Powered Binomial Array (FPBA). The main beamwidth of FPBA is much narrower, which is power efficient, than that of the popular binomial array. In [35], an approach for improvement of the binomial array antenna selectivity is studied. Ref. [36] presents the design and analysis of a large corner-fed microstrip antenna array at the C band. The side lobe level of lower than -20 dB and -14 dB in the E and H plane is achieved.

Obtaining dual-band SAA with single-layer printed circuit board (PCB) is a big challenge with SLL reduction using the binomial synthesis technique. The basic objective of this article is to design and develop an SAA technology in single-layer PCB with frequency diversity along with SLL and isolation improvement. Instead of using two separate dedicated antennas for X- and Ku-bands, SAA technology is used here. A systematic design for single linear polarization at X- and Ku-bands with high port isolation has been discussed. Realized prototypes have been experimentally investigated for binomial array distribution (BAD). The proposed design should find potential applications in SAR with frequency diversity. In this work, a low-cost and low-profile SAA antenna design prototype for X/Ku-band AIR-SAR applications is presented. The proposed antenna designs operate at X/Ku frequency bands covering 9.3/13.265 GHz. The substrate thickness of 0.787 mm with 1 oz copper cladding makes the prototypes flexible. The proposed antenna has many advantages such as: 1) low cost single layer SAA; 2) improved aperture efficiency with Single layer PCB, 3) the design features amplitude control with controlling patch width, 4) SLL reduction and gain enhancement at X/Ku-bands (it is a drawback

in multilayer SAA technology); 5) series-fed design to reduce the microstrip transmission line losses; 6) scanning capability of ±25 with grating lobe free scanning is possible.

The detailed design analysis and results for the prototype are discussed in Sections 2 and 3, respectively. The prototypes are tested using Vector Network Analyzer (VNA) for S-parameters measurements and an anechoic chamber for radiation pattern measurement in Section 4. Finally, the work is concluded in Section 5.

2. ANTENNA STRUCTURE AND DESIGN ANALYSIS

In this work, an RT/Duroid-5880 (made by Rogers) copper cladding substrate with 31 mils (0.787 mm) height, 1 oz, i.e., 0.035 mm thick copper with a relative permittivity $\varepsilon r = 2.2$ and loss tangent $\tan\delta = 0.0009$, is chosen as the antenna material [38]. All the metal components in the reported antenna design are taken to be copper with its known material parameters $\varepsilon r = 1$, $ur = 1$, and bulk conductivity $\sigma = 5.8 \times 10^7$ s/m. Table 1 describes the parameters for a dual-band linear-polarized binomial antenna array. The center frequencies for X-band and Ku-band operations are 9.3, and 13.265 GHz, respectively. The bandwidth of the two bands has to be less than 200 MHz, and the array should have linear polarizations in each band. The isolations between the linear polarizations must be greater than 25 dB. Transmitting different arrays within the same aperture is one of the challenges for linear polarization dual-band binomial array antenna, which is made up of single substrates shown in Figure 1. Arrays are designed with thickness of ground 0.035 mm, substrate RT duroid with a dielectric constant of 2.2, a substrate thickness of 0.8 mm, and a loss tangent of 0.0009. All radiating elements' broadside radiation patterns should be excited at the same phase, and antennas provide an 180° phase shift along the radiating edges. A coaxial feed is used to excite the arrays at the center element which provides the remaining 180° phase shift. Asymmetric arrays have an odd number of elements concerning the center feed elements. The overall size of the X/Ku-DBSP SAA is $200 \times 50 \times 0.8\,\text{mm}^3$ (or) $6.12 \times 1.55 \times 0.024\lambda_0$ (Free space wavelength-AIR as the medium) (or) $8.94 \times 2.236 \times 0.035\lambda_g$ (Guided wavelength-substrate material as a medium), which corresponds to the X-band center frequency 9.3 GHz, $8.845 \times 2.211 \times 0.035\lambda_0$, $12.73 \times 3.184 \times 0.05\lambda_g$, which corresponds to the Ku-band center frequency 13.265 GHz. All simulations are performed using the CST Microwave Studio student version [37]. X/Ku-band SAA element distance based on scan angle requirements on the X-axis can be calculated using Equation (1) in [25–29].

$$d_x = \frac{\lambda_x}{1 + \sin\theta_x} \tag{1}$$

where λ_x is the x-axis free-space wavelength of 9.3 GHz; d_x is the distance between the elements in the X-direction; and θ_x is the maximum scan angles of 25°.

Table 1. General specifications of X/Ku-band shared aperture antenna.

Operation bands	**X-Band**	**Ku-Band**
Centre Frequency	9.3 GHz	13.265 GHz
Polarization	Linear	Linear
Impedance bandwidth	200 MHz	200 MHz
Antenna's size	$200 \times 50 \times 0.8\,\text{mm}^3$	
Radiation Efficiency	80%	80%
Gain	13 dBi	13 dBi
Isolation	> 25 dB	> 25 dB
Side-lobe level	-15 dB	-15 dB
Scan range	25°	25°
Cross-Polarization	> 25 dB	> 25 dB
Inter-element Spacing	$0.7\lambda_0$	$0.7\lambda_0$

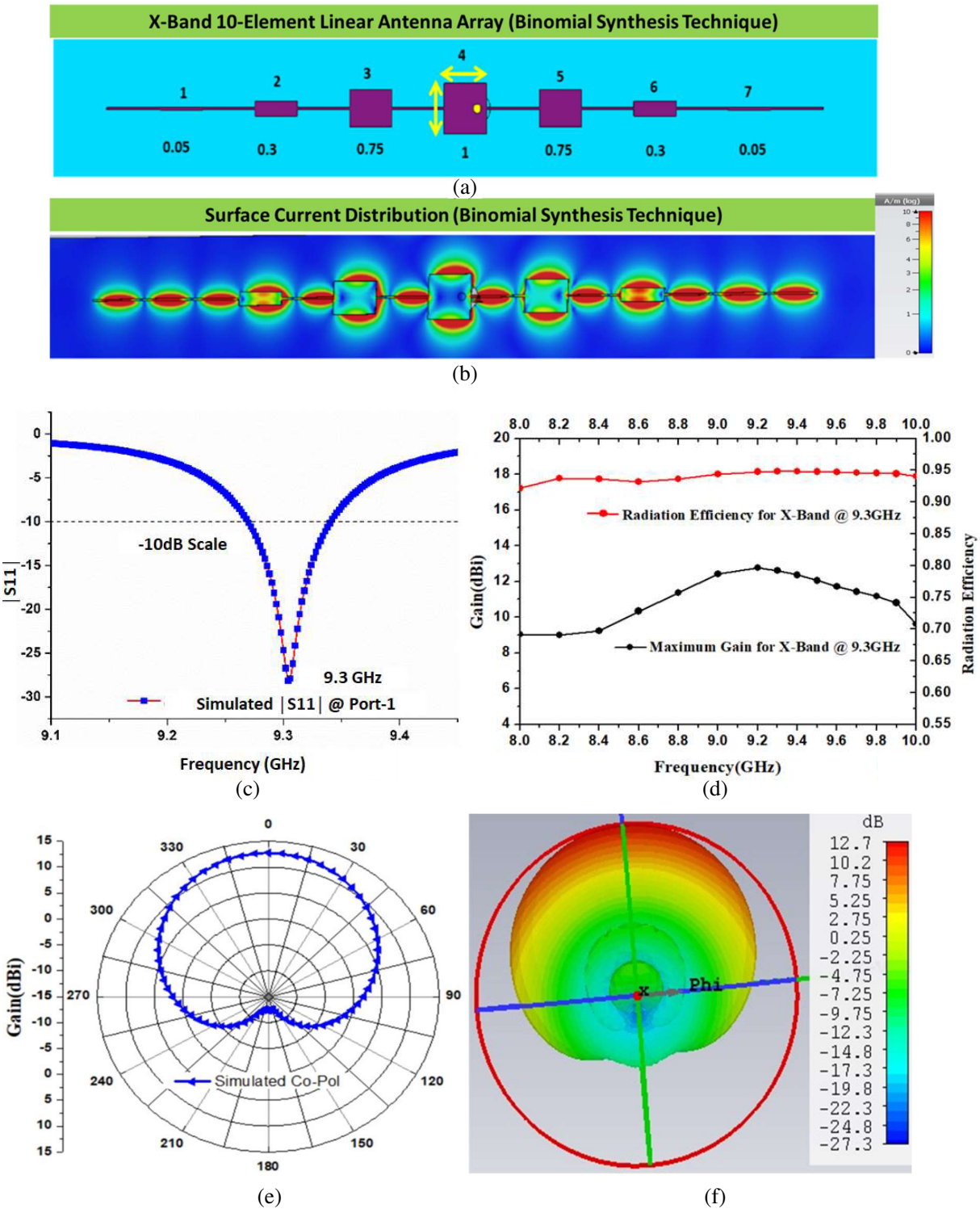

Figure 1. (a) Geometry of X-band 10-element linear antenna array with binomial synthesis technique. (b) Surface current distribution (binomial synthesis technique) of X-band 10-element linear antenna array. (c) Simulated S-parameters $|S_{11}|$ in dB at X-band. (d) Simulated gain and radiation efficiency at X-band. (e) Simulated Co-pol with zero SLL for X-band. (f) 3D radiation pattern for X-band @9.3 GHz.

General specifications of shared aperture antenna are considered as per Table 1. These specifications are going to be achieved with the proposed design. The optimized parameters of the X band and Ku band are given in Tables 2 and 3 based on amplitude values designed with the help of the binomial synthesis technique as per the design Equations (2) to (5). These final values are achieved by optimizing the design continues to get a better result.

Table 2. Optimized parameters for the X-band binomial antenna array synthesis technique.

Binomial Amplitude Distribution (X-Band @ 9.3 GHz)					
Parameter	**Description**	**Units Actual Patch Width (mm/$\lambda 0$/λg)**		**Amplitude value (watts)**	**Calculated Patch Dimensions (mm)**
$PW4$	Width of patch 4	mm	10.4	1	$1 \times 10.4 = 10.4$
		$\lambda 0$	0.322	1	$1 \times 0.322 = 0.322$
		λg	0.465	1	$1 \times 0.465 = 0.465$
$PW3 = PW5$	Width of patches 3&5	mm	10.4	0.75	$0.75 \times 10.4 = 7.8$
		$\lambda 0$	0.322	0.75	$0.75 \times 0.322 = 0.2415$
		λg	0.465	0.75	$0.75 \times 0.465 = 0.3487$
$PW2 = PW6$	Width of patches 2&6	mm	10.4	0.35	$0.35 \times 10.4 = 3.64$
		$\lambda 0$	0.322	0.35	$0.35 \times 0.322 = 0.1127$
		λg	0.465	0.35	$0.35 \times 0.465 = 0.1627$
$PW1 = PW7$	Width of patches 1&7	mm	10.4	0.05	$0.05 \times 10.4 = 0.52$
		$\lambda 0$	0.322	0.05	$0.05 \times 0.322 = 0.0161$
		λg	0.465	0.05	$0.05 \times 0.465 = 0.0023$
$PL1$ to $PL7$	Length of the Patches 1 to 7	mm	10.4		
		$\lambda 0$	0.322		
		λg	0.465		
SFL	Series Feed Length		22 mm		
SFW	Series Feed Width		0.20 mm		

In this section, the amplitudes of the radiating sources are arranged according to the coefficient of successive terms of the following binomial series in [11] of Equation (2) and hence the name

$$(a+b)^{n-1} = a^{n-1}\frac{n-1}{1!}a^{n-2}b + \frac{(n-1)(n-2)}{2!}a^{n-3}n^2 \tag{2}$$

where n denotes the number of radiating sources in the array, and a & b are the variables. For it to avoid the secondary or side lobes in the linear broadside arrays, the radiating sources must have current amplitudes proportional to the coefficient of the mentioned binomial series. This work is done by arranging the arrays so that radiating sources in the middle of the broadside array radiated more strongly than radiating sources at the borders. The secondary lobes may be eliminated. The two conditions mentioned below should be satisfied. (i) the separation between two consecutive radiating sources is smaller, and (ii) the current amplitudes in radiating sources are proportional to the coefficients of the successive terms of the binomial series. These two requirements must be met in binomial arrays, and the coefficients matching the amplitudes of the sources can be calculated by placing $n = 1, 2$. For example, in Equations (3), (4), and (5), the relative amplitudes for arrays of 1 to 7 radiating sources are as follows in [11, 31]. B_k = binomial coefficients, N = Number of Antenna elements, C_k = polynoimial expansion, K = integer.

$$C_k^{N-1} = \frac{(N-1)!}{k!(N-1-k)!} \tag{3}$$

Table 3. Optimized parameters for the Ku-band binomial antenna array synthesis technique.

Binomial Amplitude Distribution (Ku-Band @ 13.265 GHz)					
Parameter	**Description**	**Actual Patch Width (mm/$\lambda 0$/λg)**		**Amplitude value (watts)**	**Calculated Patch Dimensions (mm)**
$PW4$	Width of patch 1	mm	7.13	1	$1 \times 7.13 = 7.13$
		$\lambda 0$	0.315	1	$1 \times 0.315 = 0.315$
		λg	0.454	1	$1 \times 0.454 = 0.454$
$PW3 = PW5$	Width of patches 3&5	mm	7.13	0.75	$0.75 \times 7.13 = 5.3475$
		$\lambda 0$	0.315	0.75	$0.75 \times 0.315 = 0.2362$
		λg	0.454	0.75	$0.75 \times 0.454 = 0.3405$
$PW2 = PW6$	Width of patches 2&6	mm	7.13	0.35	$0.35 \times 7.13 = 2.4955$
		$\lambda 0$	0.315	0.35	$0.35 \times 0.315 = 0.1102$
		λg	0.454	0.35	$0.35 \times 0.454 = 0.1589$
DH $PW1 = PW7$	Width of patches 1&7	mm	7.13	0.05	$0.05 \times 7.13 = 0.3565$
		$\lambda 0$	0.315	0.05	$0.05 \times 0.315 = 0.0157$
		λg	0.454	0.05	$0.05 \times 0.454 = 0.0227$
$PL1$ to $PL7$	Length of the Patch	mm	7.13 mm		
		$\lambda 0$	0.315		
		λg	0.454		
SFL	Series Feed Length		15.4 mm		
SFW	Series Feed Width		0.20 mm		

*SFL = Series-fed line Length, SFW = Series-fed line Width. PL = Patch Length, PW = Patch width

$$B_k = \frac{C_k^{N-1}}{C_{\frac{N-1}{2}}^{N-1}} \tag{4}$$

$$B_k = \begin{matrix} 1 & 6 & 15 & 20 & 15 & 6 & 1 \\ \frac{C_0^6}{C_3^6} & \frac{C_1^6}{C_3^6} & \frac{C_2^6}{C_3^6} & \frac{C_3^6}{C_3^6} & \frac{C_4^6}{C_3^6} & \frac{C_5^6}{C_3^6} & \frac{C_6^6}{C_3^6} \\ 0.05 & 0.3 & 0.75 & 1 & 0.75 & 0.3 & 0.05 \end{matrix} \tag{5}$$

$$k = 0, 1, 2, 3, 4, 5, 6, 7 \ldots N-1$$

2.1. X-Band 7-Element SFCFOS Linear Antenna Array with Binomial Synthesis Technique

The binomial array is designed at a frequency of 9.3 GHz for X band, patch width tapering geometry of a seven-element SFCFOS binomial array. Table 2 shows the optimized parameters of the X-band binomial antenna array synthesis technique. In the SFCFOS array design, binomial synthesis techniques are chosen to provide the SLL of > -40 dB in practice. To obtain a flat SLL performance, we use amplitude coefficients modified from a binomial synthesis and introduce a half-wavelength open-ended stub after the last element for the effective utilization of transmitted power. The width of the center patch is

10.4 mm. The patch width of the other elements is variable, with a ratio of 1, 0.75, 0.35, and 0.05 from the array center to the edges. The distance between two adjacent elements is 22 mm ($0.7\lambda_0$ at 9.3 GHz). The radiating elements' physical length and width of the X-band were determined as $L1 = L7 = 10.4$ m and $W4 = 10.4$ mm, $W3 = W5 = 7.8$ mm, $W2 = W6 = 3.64$ mm, $W1 = W7 = 0.52$ mm, and series feed length (SFL) and series feed width (SFW) are 22 mm and 0.2 mm. The series-fed X-band array has a SFW that is optimized to 0.2 mm. The typical inter-element spacing employed in the X-band array is in the range of 0.7λ, which corresponds to the center frequency 9.3 GHz (approximately one-guided wavelength), SFL = 22 mm in this X-band linear array. The coefficient of the binomial array distribution was designed for N number of odd elements. From the central element to the end element, the excitation amplitude can be decreased from arrays and current distribution as shown in Figure 1(b). The amplitude is controlled by varying the width of the microstrip patch elements, and open-ended stubs are arranged next to the last antenna element to use the energy of the radiating signal more effectively. The coaxial probe is fed into the central element at a distance from its center for impedance matching. Simulated bandwidth (BW) for $|S_{11}| \leq -10$ dB is from 9.25 to 9.35 GHz (1.07%) and return loss is 25 dB at 9.3 GHz which are shown in Figure 1(c). Figure 1(d) shows the simulated gain and radiation efficiency with achieved value of 12.8 dBi and 92.5%, respectively. The polar representation of radiation patterns with zero SLLs and 3D radiation patterns are shown in Figures 1(e) & (f).

2.2. Ku-Band 7-Element SFCFOS Linear Antenna Array with Binomial Synthesis Technique

The binomial array is designed with a frequency of 13.265 GHz for Ku-band with a seven-element SFCFOS as shown in Figure 2(a). Table 3 shows the optimized parameters of the Ku-band binomial antenna array synthesis technique. In the SFCFOS array design, binomial synthesis techniques are chosen to provide the SLL of > -40 dB in practice. To obtain a flat SLL performance, we use amplitude coefficients modified from a binomial synthesis and introduce a half-wavelength open-ended stub after the last element for effective utilization of transmitted power. The width of the center patch is 10.4 mm. The patch width of the other elements is variable, with ratios of 1, 0.75, 0.35, and 0.05 from the array center to the edges. The radiating element length and width in Ku-band were chosen as $L1 = L7 = 7.13$ mm and $w4 = 7.13$ mm, $w3 = w5 = 5.34$ mm, $w2 = w6 = 2.49$ mm, $w1 = w7 = 0.35$ mm, and SFL and SFW are 8 mm and 0.8 mm. The typical inter-element spacing employed in the Ku-band array is in the range of 0.7λ, which corresponds to center frequency 13.265 GHz (approximately one-guided wavelength), SFL = 20 mm in this X-band linear array. From the central element to the end element, the excitation amplitude can be decreased from arrays and current distribution as shown in Figure 2(b). The amplitude is controlled by varying the width of the microstrip patch elements, and open-ended stubs are arranged next to the last antenna element to use the energy of the radiating signal more effectively. The coaxial probe is fed into the central element at a distance from its center for impedance matching. Simulated BW for $|S_{11}| \leq -10$ dB is from 13.15 to 13.35 GHz (1.5%), and return loss is -15.7 dB at 13.265 GHz which are shown in Figure 2(c). Figure 2(d) shows the simulated gain and radiation efficiency with achieved values of 13.2 dBi and 91%. The polar representation of radiation patterns with zero SLLs and 3D radiation patterns are shown in Figures 2(e) & (f).

3. EMBEDDING X/KU DBSP BINOMIAL SHARED APERTURE ANTENNA

The geometry configurations of the proposed X/Ku-band SAA with all dimensions are shown in Figure 3(a). The array consists of 7 elements arranged in a linear array configuration with a series-fed center-fed open stub design method. The series-fed X/Ku-band array has a feed width (SFW) that is optimized to 0.8 mm. The typical inter-element spacing employed in the X-band array is in the range of 0.7λ, which corresponds to center frequency 9.3 GHz (approximately one-guided wavelength), SFL = 22 mm in this SAA X/Ku-band linear array. Optimal spacing is used to save the number of antenna elements for a narrow beamwidth and directivity. The element distance is restricted by scan requirement factors. To obtain a flat SLL performance, we use amplitude coefficients modified from a binomial synthesis and introduce a half-wavelength open-ended stub after the last element for the

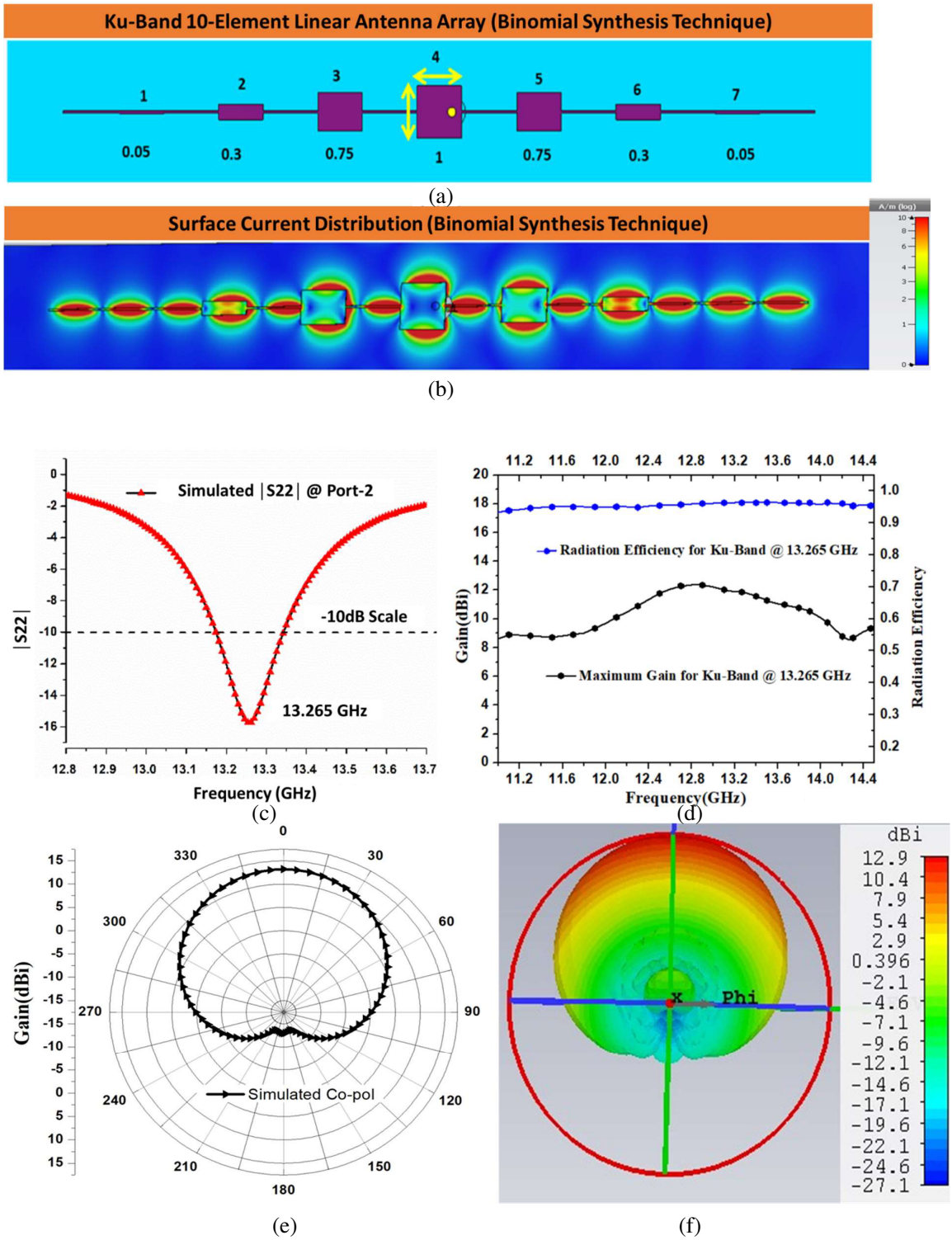

Figure 2. (a) Geometry of Ku-band 10-element linear antenna array with binomial synthesis technique. (b) Surface current distribution (binomial synthesis technique) of Ku-band 10-element linear antenna array. (c) Simulated S-parameters $|S_{22}|$ in dB at Ku-band. (d) Simulated gain and radiation efficiency at Ku-band. (e) Simulated Co-pol with zero SLL for Ku-band. (f) 3D radiation pattern at Ku-band.

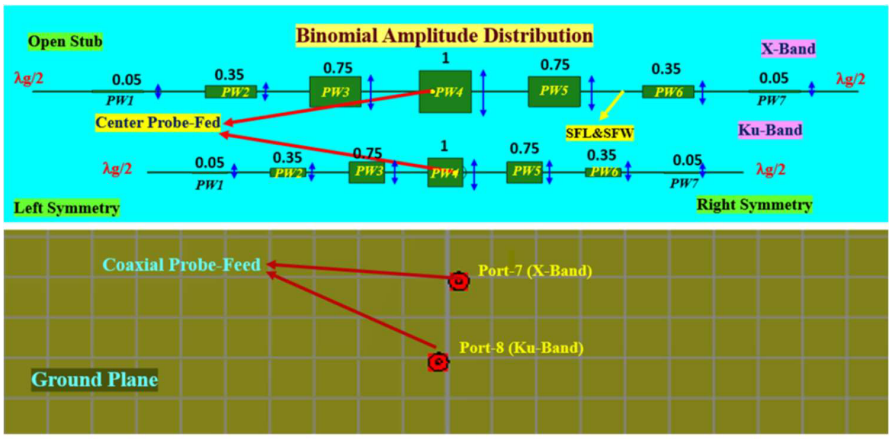

(a)

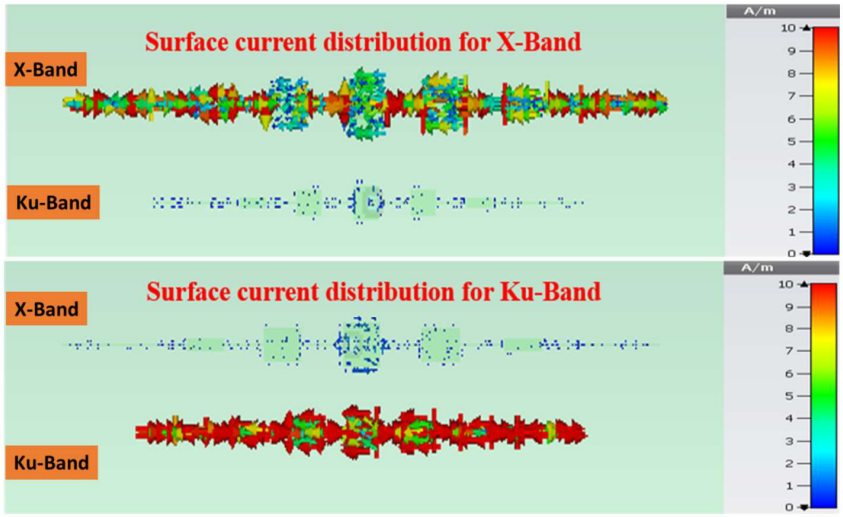

(b)

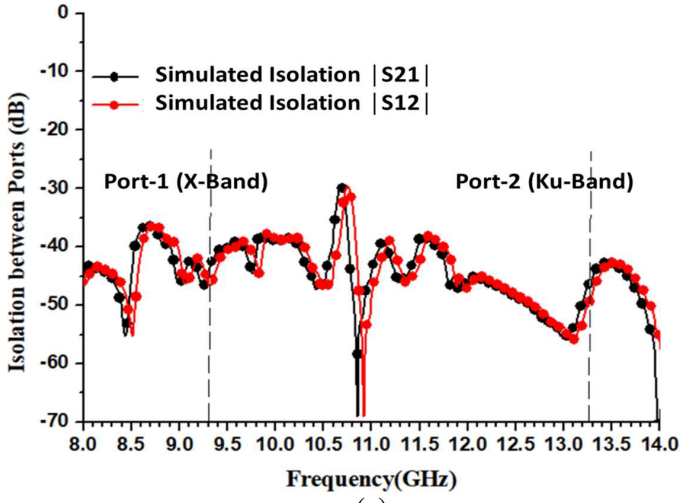

(c)

Figure 3. (a) Geometry of shared aperture antenna X/Ku-band binomial array. (b) Surface current distribution of X/Ku-band binomial array. (c) Simulated isolation between ports for X/Ku-band binomial array.

effective utilization of transmitted power. The X/Ku band SAA design has been adopted to reduce the payload weight, size, and cost. To improve the isolation (reduce the mutual coupling between the X/Ku-band SAAs) between the ports (i.e., Port-1 & Port-2) or X/Ku-band SAAs, the array distance considered was greater than 0.5λ at the lowest operating frequency which can be shown as a surface current distribution when one of the ports was excited in Figure 3(b). The isolation $|S_{21}|$ & $|S_{12}|$ between ports are greater than -45 dB at port-1 and port-2 and are shown in Figure 3(c).

4. SIMULATED AND EXPERIMENTAL RESULTS AND ANALYSIS

The X/Ku-band binomial shared-aperture array prototype, with central frequencies of 9.3 GHz and 13.265 GHz for X- and Ku-bands, respectively, are fabricated and measured to validate the design. As shown in Figures 4(a)–(b), the prototype array is incorporated with X/Ku-bands. The S-parameters and radiation patterns are measured using Keysight-E5063A (100 kHz–14 kHz) ENA Series Network Analyzer as shown in Figure 4(c), and the radiation patterns and gain measurements are measured in an anechoic chamber. The measurement setups for both S-parameters and radiation patterns are shown in Figures 4(d)–(e).

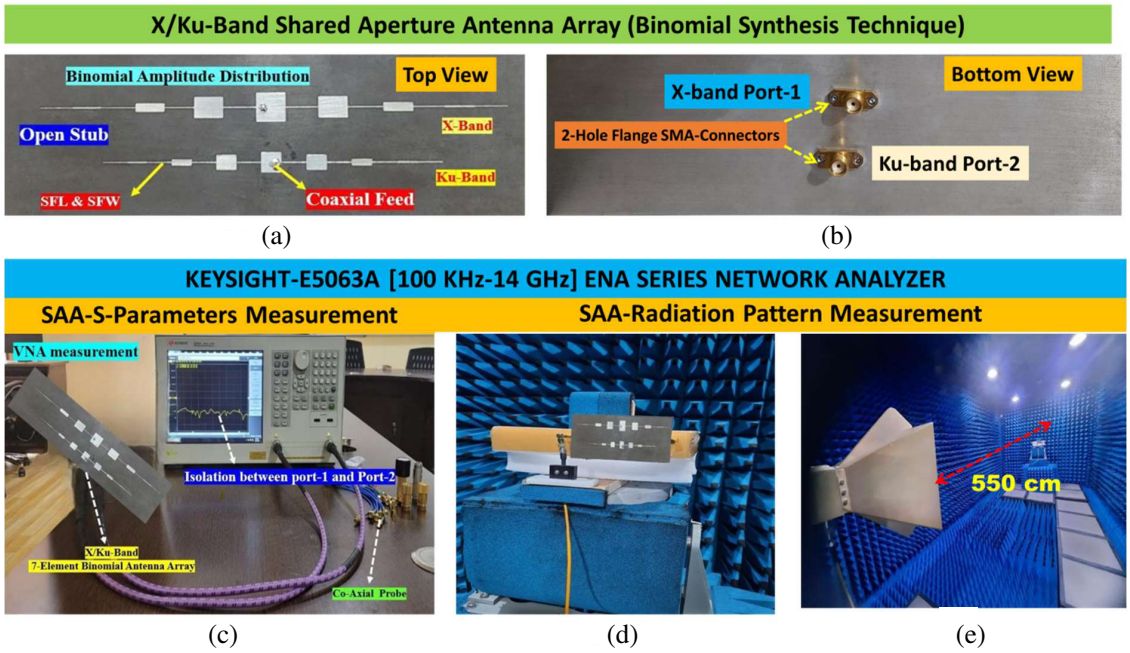

Figure 4. Fabricated prototype. (a) Top and (b) bottom view photograph of X/Ku-band binomial SAA. (c) S-parameters measurement setup. (d) & (e) Radiation pattern measurement setup with standard gain horn.

The measured return loss S_{11} of the proposed X/Ku-band binomial SAA is presented in Figure 5(a). The results show measured return loss or impedance bandwidth of 9.23–9.36 GHz (1.07%) at X-band and 13.15–13.35 GHz (1.5%) at Ku-band with a resonant frequency of 3.2 GHz and 9.3 GHz, respectively. The results agree well with simulated and measured antenna parameters. Isolation higher than 45 dB in both X- and Ku-bands is obtained. Figure 5(b) gives the simulated and measured isolation results between X/Ku-bands. The notations of X-band port is port-1, and port-2 refers to Ku-band array.

Radiation patterns of the antenna system are measured at both X- and Ku-bands as shown in measurement setup in an anechoic chamber and are displayed in Figures 6(a) & (b). Measured radiation patterns of the X-band antenna at port-1 at 9.3 GHz are two orthogonal planes (E-plane/Phi $= 0°$ & H-plane/Phi $= 90°$) and are shown in Figures 6(a)–(b). Measured radiation patterns of the Ku-band antenna at port-2 at 13.265 GHz are two orthogonal planes (E-plane/Phi $= 0°$ & H-plane/Phi $= 90°$)

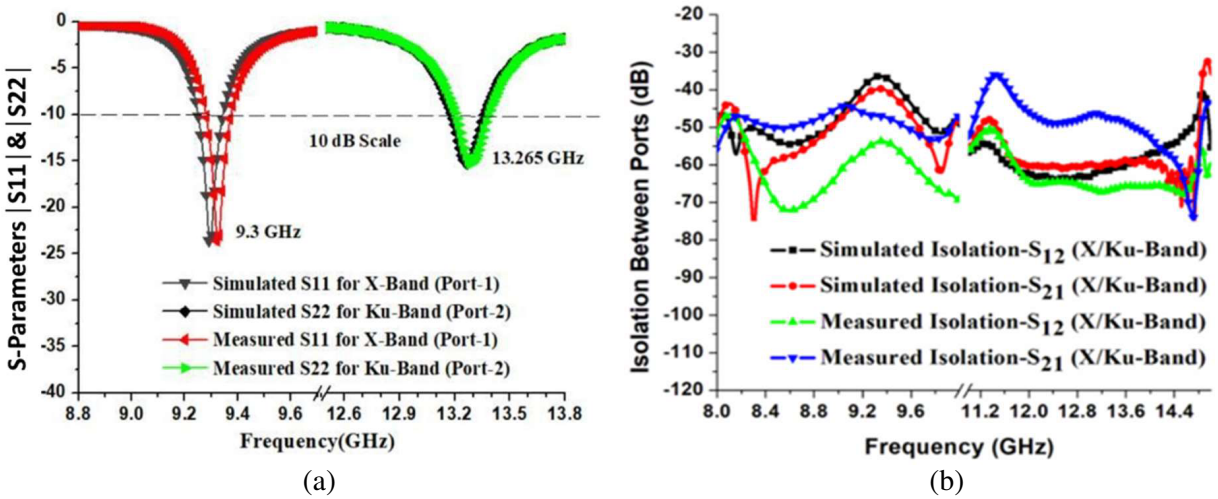

Figure 5. (a) Simulated and measured S-parameters ($|S_{11}|$ & $|S_{22}|$ of X/Ku-band binomial SAA. (b) Simulated and measured isolation between bands of the X/Ku-band binomial SAA.

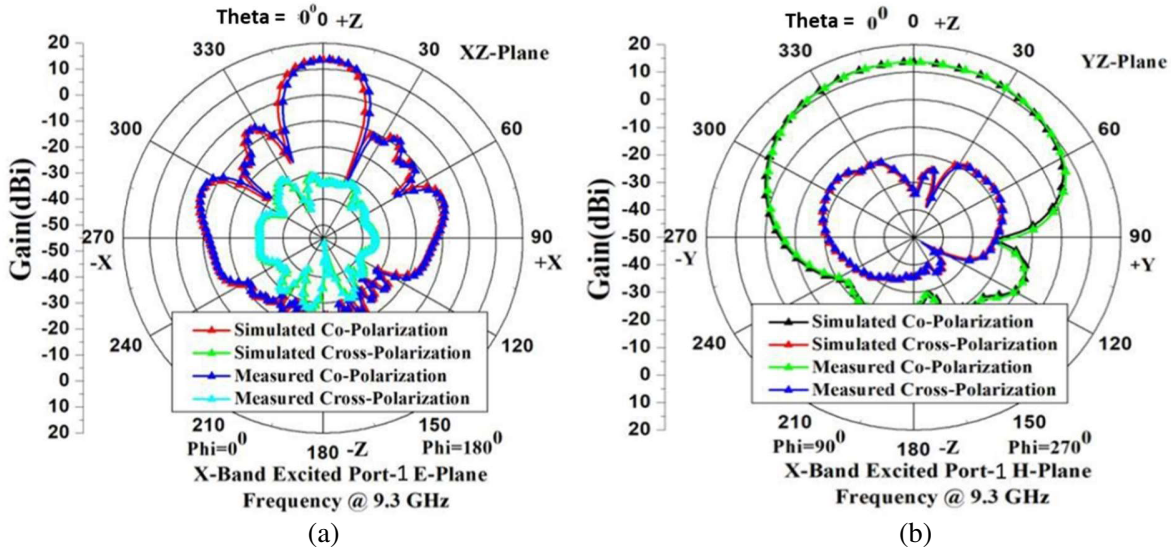

Figure 6. Simulated and measured radiation patterns of the X/Ku-band shared aperture antenna at 9.3 GHz: (a) E-plane, Port-1 excitation; (b) H-plane, Port-1 excitation.

and are shown in Figures 1(a)–(d). Good agreement between the simulated and measured results is obtained with directional characteristics. It can be found that the peak radiation happens in the broadside direction at these two frequencies. The cross-polarization level at 9.3 GHz in the E- & H-planes is below -28 dB/-26 dB. The cross-polarization level at 13.265 GHz in the E- & H-planes is below -26 dB/-27 dB. The measured SLL is less than -15.9/-39 dB in both E- & H-planes at 9.3 GHz. At 13.265 GHz, the SLL remains below -17.4 and -36.1 dB in the E- & H-planes.

The distance between the transmitting antenna and receiving antennas is in the far-field region as shown in Equation (6) in [11]. The radiation pattern is measured in an anechoic chamber using a standard gain horn antenna as the reference antenna having a gain (Gr) of 10 dBi at X/Ku-band. The reference antenna and proposed antenna are kept at a distance (R) of 550 cm. The power received by the horn antenna is 30 dBm for both cases, and the power received by the antenna under test (AUT) is around 28 dBm for X-band and -18.7 dBm for Ku-band. The transmitted power (Pt) is 0 dBm.

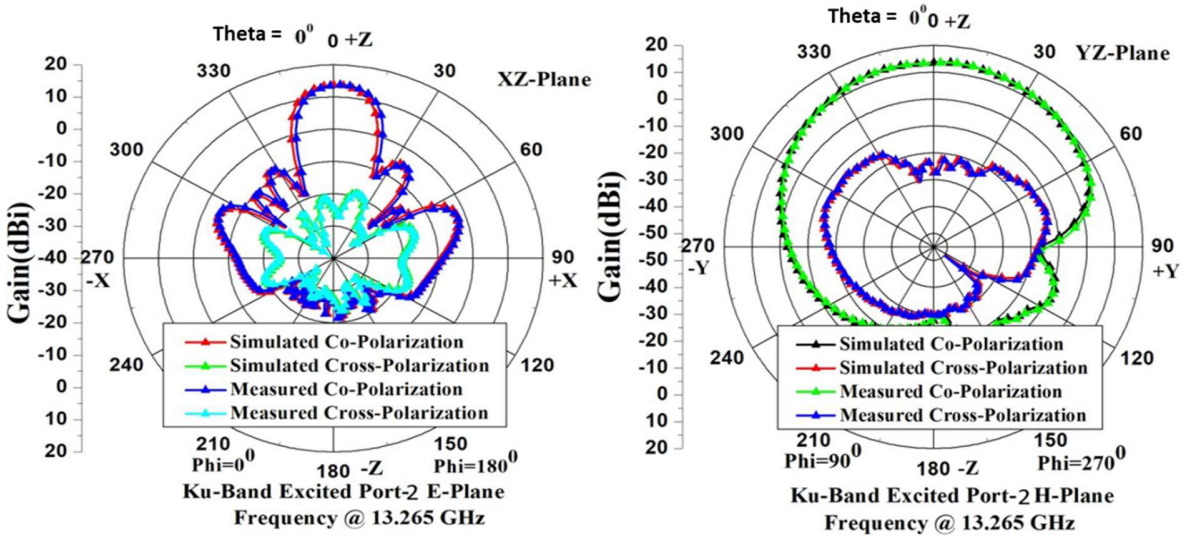

Figure 7. Simulated and measured radiation patterns of the X/Ku-band shared aperture antenna at 13.265 GHz: (a) E-plane, Port-2 excitation; (b) H-plane, Port-2 excitation.

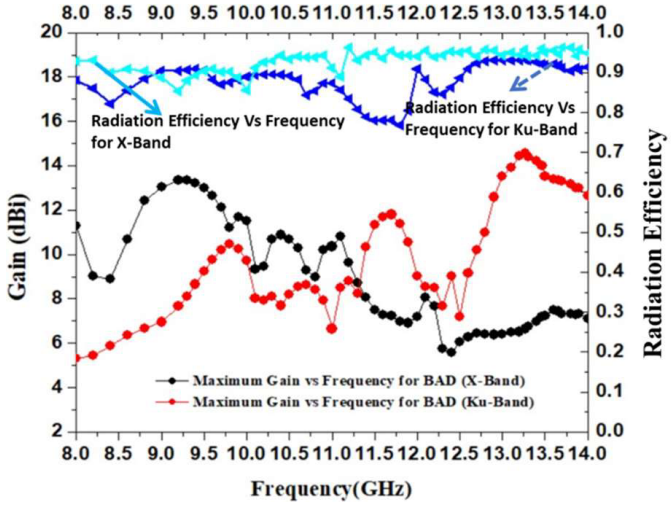

Figure 8. Simulated and measured gain and radiation efficiency for X/Ku-band binomial SAA.

The received power (Pr) is 30 dBm at X-band/Ku-band. The gain of the antenna under test (Gt) is calculated using the Friis transmission equation as follows in Equation (5) in [11].

$$r > 2D^2/\lambda \tag{6}$$

$$P_r = P_t G_r G_r \left(\frac{\lambda^2}{4\pi R}\right) \tag{7}$$

Figures 6(a)–(b) show the simulated and measured X-band radiation patterns at 9.3 GHz. The antenna radiates well on the broadside. A 50 load on port 1 (X-band linear polarization) gives P1 a half-power beamwidth of 86.8° and a 12.8 dBi gain. The half-power beamwidth of 20.5° and a gain of 12.7 dBi are observed in the E-plane. Both planes have an front to back ratio (FTBR) of 18 dB or higher. Figures 7(a)–(b) show the simulated and measured experimental Ku-band antenna radiation patterns at 13.265 GHz. The antenna has good half-power bandwidth (HPBW) and gains due to the increase in

Table 4. Summary of the X/Ku-band binomial SAA S-parameters and radiation characteristics.

Parameter		X-Band (9.3 GHz)		Ku-Band (13.265 GHz)	
		Simulated	Measured	Simulated	Measured
Impedance Bandwidth		9.23–9.36	9.25–9.36	13.15–13.35	13.15–13.35
Isolation Between bands		> 40 dB			
Gain		12.8	12.7	13.2	13.2
Radiation efficiency		92.5	93	91	91
E-Plane	SLL (dB)	-39.5	-39	-35	-36.1
	HPBW (deg)	86.8	20.5	77.9	21.3
	X-pol (dB)	-28	-26	-26	-26
	FTBR (dB)	18	17.4	18	18.1
H-Plane	SLL (dB)	-15.9	-17.9	-17.4	-19
	HPBW (deg)	20.5	86.8	21.3	77.9
	X-pol (dB)	-28.1	-26.1	-19	-24
	FTBR (dB)	18	18.2	18	17.8
Aperture area (Ap)		$200 \times 50 \times 0.787\,\text{mm}^3$			
Effective area (Ae)		$165 \times 11\,\text{mm}^2$		$120 \times 7\,\text{mm}^2$	
Aperture efficiency (ea)		18.15%		8.4%	
Note: For X-band 7-element binomial array is 18.15% For S-band the utilization effective area is 8.4% Efficient utilization of X/Ku-band Binomial SAA is 26.9%					

Table 5. Comparison with other SA.

S.-No.	Band-1/ Band-2	Resonance Frequency GHz	configuration	Gain dBi	Cross-pol dB	Isolation dB	SLL (dB)	Scan angle	Application
[13]	S/X	8.55 to 9.6	Multilayer 8×16	7.6 dBi	NA	35 dB	NA	$\pm 50°$	Wireless Application
[14]	Ku/Ka	14.2–18/ 31.0–33.6 GHz	Multilayer Phased Array $2 \times 3/4 \times 4$	8.4 dBi/ 9 dBi/ 8.7 dBi	8.4 dBi/ 9 dB/ 8.7 dB	15 dB	-17 dB/ -13 dB	$\pm 25°$	Wireless Application
[15]	S/C	2.12–2.75/ 5.69–5.91	Multilayer Phased Array 6×6	7.9 dBi/ 2.7 dBi/ 11.7 dBi	7.9 dBi/ 2.7 dB/ 11.7 dB	43/25 dB	NA	$\pm 25°$	Satellite Communication
[16]	Ku/Ka	13/38 GHz	Multilayer	28.2/ 37.2 dBi	28.2/ 37.2 dB	> 30 dB	NA	$\pm 25°$	Satellite Communication
[17]	S/C	2.4/ 5.8 GHz	Multilayer 4×4	11.7 dBi	11.7 dB	30 dB	-12 dB (both)	$\pm 25°$	Wireless Application
[18]	Ku/Ka	16/35 GHz	Multilayer $8 \times 8/8 \times 8$	22.3 dBi/ 22.1 dBi.	-22 dB	> 30 dB	NA	$35°$/ $40°$/ $50°$/ $60°$	Satellite Communication
[19]	S/L	3.4–3.8/ 0.69–0.96 GHz	Multilayer	7.3/ 13 dBi	> 20/ > 15 dB	> 30 dB/ > 25 dB	NA	$\pm 25°$	future 5G Application
[20]	Ka	28 GHz	Single layer 1×4	9.56-dBi/ 8.9 dBi	3.23 dB	32 dB	NA	$\pm 45°$	MIMO Application
[21]	Ku/Ka	16 GHz/ 33.5 GHz	Multilayer 1×4	18.4/ 18 dBi	18.4/ 23.4 dB	15 dB	NA	$\pm 25°$	Satellite Communication
[22]	K/Ka	17.7–21.2/ 27.5–31.0 GHz	Multilayer	4.5 dBi	4.5 dB	40 dB	-7 dB (both)	$\pm 60°$	LEO Satellite Communication
This work (Binomial SAA)	X/Ku	9.3/13.265	Linear Array (single layer)	12.8/ 13.2	-28/ -26 dB	> 45 dB	-39 dB/ -35 dB	$\pm 25°$	SAR Application

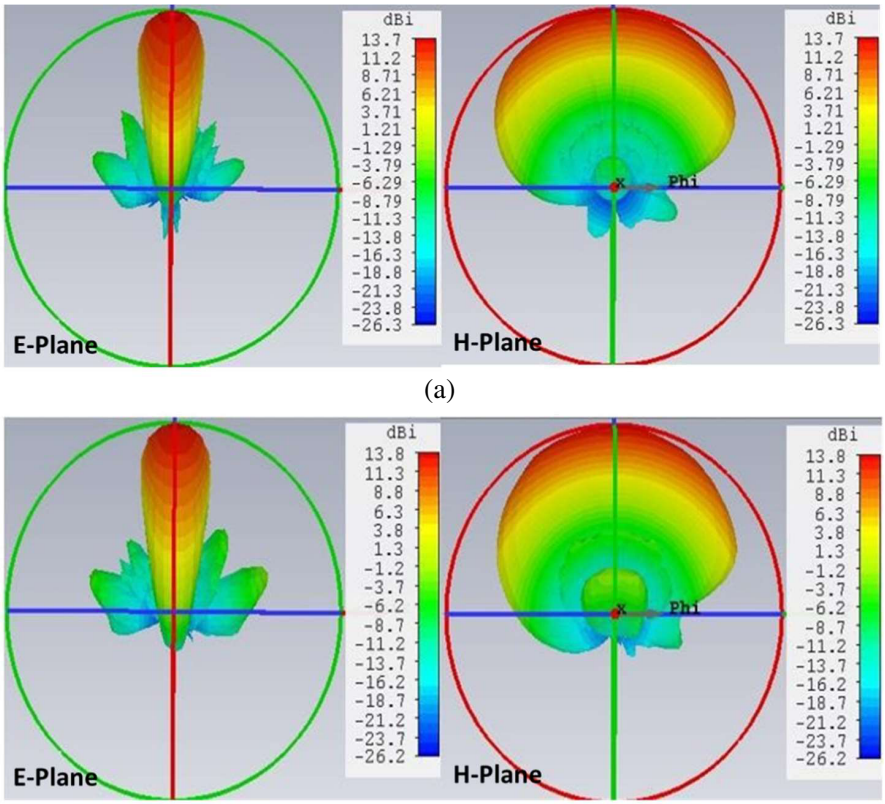

Figure 9. (a) Simulated far-field gain for $\phi = 0°$ (E-plane), $\phi = 90°$ (H-plane) at 9.3 GHz. (b) Simulated far-field gain for $\phi = 0°$ (E-plane), $\phi = 90°$ (H-plane) at 13.265 GHz.

electrical size at high-band. The P1 is terminated with a 50 load for Ku-band linear polarization (P2). The antenna's HPBW is 21.3°, and its gain is 13.2 dBi. The HPBW is 77.9°, and the gain is 13.2 dBi. FTBR > 18 dB in both planes.

A standard gain horn antenna is utilized as a reference antenna during the measurement of the gains. Figure 8 shows the simulated and measured realized gain/efficiencies of this antenna. Peak gain is 12.8 dBi at 9.3 GHz, equivalent to efficiencies of 92.5/93%. In the Ku-band, maximal linear polarization gains are around 13.2 dBi at 13.265 GHz, equivalent to efficiencies of 91% at both the planes. Figure 9 depicts 3D radiation patterns. The X/Ku-band SAA S-parameters and radiation properties, such as bandwidth, gain radiation efficiency, SLL, HPBW, and cross-pol, are determined and summarized in Table 4.

A single-layer antenna array is an element array in X and Ku bands. Compared to the SAAs in [13–22], the suggested SAA has an FR of 1.426, better gains, and better band isolation. The dual-band prototype has a compact, single-layer, linear binomial SAA architecture. Table 5 compares the SAA design to different SAA designs. We confirm an SAA design with reasonable performance. This design can be used to determine the best literary work.

5. CONCLUSION

This research paper proposes a novel dual-band single-polarized (DBSP) series-fed center-fed open stub (SFCFOS) Binomial Antenna Array synthesis technique to improve side lobe level (SLL) and better isolation for the use in Airborne Synthetic Aperture Radars (AIR-SARs). The prototype is fabricated and tested for S-parameters, radiation characteristics, and gain measurements. The measured results of the prototype align well with the simulated ones, exhibiting excellent radiation performance and high

isolation. The bandwidth of 1.07% (X-band) and 1.5% (Ku-band) and return loss of 25 dB/−15.7 dB at 9.3/13.265 GHz are achieved. The measured isolation is −45 dB which provides a large signal separation at X/Ku-bands. The antenna design shows a side-lobe level (SLL) of −39.5 dB at E-plane ($\varphi = 0°$) and −17.9 dB for H-plane ($\varphi = 90°$) for the X-band and −35 dB at $\varphi = 0°$ −19 dB for H-plane ($\varphi = 90°$) for the Ku-band. Additionally, the proposed SAA has high gain values of 12.8 dBi for the X-band and 13.2 dBi for the Ku-band. The size of the shared-aperture antenna is 200 mm × 50 mm × 0.787 mm. The SAA is best suited for large-size array antennae for SAR applications. The proposed SAA has many advantages, such as a single-layer structure, easy fabrication, low production cost, and good isolation between the bands and between the polarizations. The proposed X/Ku band binomial SAA is also suitable for the synthesis of the array, which holds significant value for AIR-SAR applications.

ACKNOWLEDGMENT

This work has been carried out at the Centre of Excellence Advanced RF Microwave & wireless communications. The authors thank Rogers Corporation, USA for their support in providing RT Duroid 5880 samples for academic research purposes. The Author Dr. Venkata Kishore Kothapudi would like to thank the director Dr. Ravi Sekhar Yarrabothu and the In-charge Dr. Pachiyaannan Muthusamy of our COE for their tremendous support in facilitating the timely requirements for the execution of this research work. We thank Mr. Ravi Kumar Dasari (for his support during fabrication and assembling), Department of Electronics Communication Engineering (ECE), School of Electrical, Electronics, and Communication Engineering, Vignan's Foundation for Science, Technology, and Research (Deemed to be University), Vadlamudi, Guntur District, Andhra Pradesh, India-522213. Authors thank manuscript reviewers.

REFERENCES

1. Moreira, L., P. Prats-Iraola, M. Younis, G. Krieger, I. Hajnsek, and K. Pa-Athanasiou, "A tutorial on synthetic aperture radar," *IEEE Geoscience and Remote Sensing Magazine (GRSM)*, Vol. 1, 6–43, Mar. 2013.
2. Skolnik, M. I., *Radar Handbook*, 3rd Edition, 1.1–24.1, McGraw-Hill, New York, 1970.
3. Drinkwater, M. R., R. Kwok, and E. Rignot, "Synthetic aperture radar polarimetry of sea ice," *Digest — International Geoscience and Remote Sensing Symposium (IGARSS)*, Vol. 2, 1525–1528, 1990.
4. Lynne, G. J. and G. R. Taylor, "Geological assessment of SIRB imagery of the Amadeus basin, N.T., Australia," *IEEE Trans. Geosci. Remote Sens.*, Vol. 24, No. 4, 575–581, 1986.
5. Hovland, H. A., J. A. Johannessen, and G. Digranes, "Slick detection in SAR images," *International Geoscience and Remote Sensing Symposium (IGARSS)*, Vol. 4, 2038–2040, 1994.
6. Walker, B., G. Sander, M. Thompson, B. Burns, R. Fellerhoff, and D. Dubbert, "High-resolution, four-band SAR testbed with real-time image formation," *International Geoscience and Remote Sensing Symposium (IGARSS)*, Vol. 3, 1881–1885, 1996.
7. Storvold, R., E. Malnes, Y. Larsen, K. A. Hogda, S. E. Hamran, K. Müller, and K. A. Langley, "SAR remote sensing of snow parameters in Norwegian areas — Current status and future perspective," *Journal of Electromagnetic Waves and Applications*, Vol. 20, No. 13, 1751–1759, 2006.
8. Kong, J. A., S. H. Yueh, H. H. Lim, R. T. Shin, and J. J. van Zyl, "Classification of earth terrain using polarimetric synthetic aperture radar images," *Progress In Electromagnetic Research*, Vol. 3, 327–370, 1990.
9. Jordan, R. L., B. L. Huneycutt, and M. Werner, "The SIR-C/X-SAR synthetic aperture radar system," *IEEE Trans. Geosci. Remote Sens.*, Vol. 33, No. 4, 829–839, 1995.
10. Axness, T. A., R. V. Coffman, B. A. Kopp, and K. W. O'Haver, "Shared aperture technology development," *Johns Hopkins APL Tech. Dig.*, Vol. 17, No. 3, 285–293, 1996.
11. Balanis, C. A., *Antenna Theory: Analysis and Design. Antennas & Propagation*, 4th Edition, Wiley, Hoboken, 1997.

12. Zhong, S.-S., Z. Sun, L.-B. Kong, C. Gao, W. Wang, and M.-P. Jin, "Tri-band dual polarization shared-aperture microstrip array for SAR applications," *IEEE Transactions on Antennas and Propagation*, Vol. 60, 4157–4165, Sep. 2012.
13. Zhou, C., S. Yuan, H. Li, B. Wang, and H. Wong, "Dual-band shared-aperture antenna with bifunctional metasurface," *IEEE Antennas and Wireless Propagation Letters*, Vol. 20, No. 10, 2013–2017, 2021.
14. Liu, Y., Y. J. Cheng, and Y. Fan, "A dual-layer Ku/Ka dual-band shared-aperture reflectarray antenna based on structure-reuse technique," *2021 IEEE International Symposium on Antennas and Propagation and USNC-URSI Radio Science Meeting (APS/URSI)*, 1925–1926, 2021.
15. Bai, C. X., Y. J. Cheng, Y. R. Ding, and J. F. Zhang, "A metamaterial-based S/X-band shared-aperture phased-array antenna with wide beam scanning coverage," *IEEE Transactions on Antennas and Propagation*, Vol. 68, No. 6, 4283–4292, 2020.
16. Liu, L. Y., Y. J. Cheng, and L. Wang, "Dual-polarized Ku-band and single-polarized Ka-band shared-aperture phased array antenna," *2021 International Conference on Microwave and Millimeter Wave Technology (ICMMT)*, 1–3, May 2021.
17. Y. R. Ding, Y. J. Cheng, J. X. Sun, L. Wang, and T. J. Li, "Dual-band shared-aperture two-dimensional phased array antenna with wide bandwidth of 25.0% and 11.4% at Ku- and Ka-band," *IEEE Transactions on Antennas and Propagation*, Vol. 70, No. 9, 7468–7477, Sep. 2022.
18. Niu, W., B. Sun, G. Zhou, and Z. Lan, "Dual-band aperture shared antenna array with decreased radiation pattern distortion," *IEEE Transactions on Antennas and Propagation*, Vol. 70, No. 7, 6048–6053, Jul. 2022.
19. Ou, J.-H., B. Xu, S. F. Bo, Y. Dong, S.-W. Dong, and J. Tang, "Highly-isolated RF power and information receiving system based on dual-band dual-circular-polarized shared-aperture antenna," *IEEE Transactions on Circuits and Systems I: Regular Papers*, Vol. 69, No. 8, 3093–3101, Aug. 2022.
20. Kim, B., M. Kim, D. Lee, J. Lee, Y. Youn, and W. Hong, "A shared-aperture cavity slot antenna-in-package concept featuring end-fire and broadside radiation for enhanced beam coverage of mmwave mobile devices," *IEEE Transactions on Antennas and Propagation*, Vol. 71, No. 2, 1378–1390, Feb. 2023.
21. Ran, J., Y. Wu, C. Jin, P. Zhang, and W. Wang, "Dual-band multipolarized aperture-shared antenna array for Ku-/Ka-band satellite communication," *IEEE Transactions on Antennas and Propagation*, Vol. 71, No. 5, 3882–3893, May 2023.
22. Hao, R. S., J. F. Zhang, S. C. Jin, D. G. Liu, T. J. Li, and Y. J. Cheng, "K-/Ka-band shared-aperture phased array with wide bandwidth and wide beam coverage for LEO satellite communication," *IEEE Transactions on Antennas and Propagation*, Vol. 71, No. 1, 672–680, Jan. 2023.
23. Li, K., T. Dong, and Z. Xia, "A broadband shared-aperture L/S/X-band dual polarized antenna for SAR applications," *IEEE Access*, Vol. 7, 51417–51425, 2019.
24. Yang, G.-W. and S. Zhang, "A dual-band shared-aperture antenna with wide-angle scanning capability for mobile system applications," *IEEE Trans. Veh. Technol.*, Vol. 70, No. 5, 4088–4097, May 2021.
25. Kothapudi, V. K. and V. Kumar, "A multi-layer S/X-band shared aperture antenna array for airborne synthetic aperture radar applications," *International Journal of RF and Microwave Computer-Aided Engineering*, Vol. 31, No. 8, e22720, 2021.
26. Kothapudi, V. K. and V. Kumar, "SFCFOS uniform and Chebyshev amplitude distribution linear array antenna for K-band applications," *Journal of Electromagnetic Engineering and Science*, Vol. 19, 64–70, Jan. 2019.
27. Kothapudi, V. K. and V. Kumar, "Hybrid-fed shared aperture antenna array for X/K-band airborne synthetic aperture radar applications," *IET Microwaves, Antennas & Propagation*, Vol. 15, Dec. 2020.

28. Kothapudi, V. K. and V. Kumar, "A 6-port two-dimensional 3×3 series-fed planar array antenna for dual-polarized X-band airborne synthetic aperture radar applications," *IEEE Access*, Vol. 6, 12001–12007, Mar. 2018.
29. Kothapudi, V. K. and V. Kumar, "Compact 1×2 and 2×2 dual polarized series-fed antenna array for X-band airborne synthetic aperture radar applications," *Journal of Electromagnetic Engineering and Science*, Vol. 18, 117–128, Apr. 2018.
30. Chopra, R. and G. Kumar, "Series-fed binomial microstrip arrays for extremely low sidelobe level," *IEEE Transactions on Antennas and Propagation*, Vol. 67, No. 6, 164275–164279, 2019.
31. Mishra, N. K. and S. Das, "Investigation of binomial and Chebyshev distributionon dielectric resonator antenna array," *Processing, and Computing Technologies*, 434–437, 2014.
32. Mathur, P., G. Kumar, P. K. Mishra, and Y. K. Verma, "Large gain linear series-fed microstrip antenna arrays at Ka and C bands," *2015 IEEE International Symposium on Antennas and Propagation & USNC/URSI National Radio Science Meeting*, 1872–1873, Vancouver, BC, Canada, 2015.
33. Chopra, R. and G. Kumar, "Series- and corner-fed planar microstrip antenna arrays," *IEEE Transactions on Antennas and Propagation*, Vol. 67, No. 9, 5982–5990, 2019.
34. Baki, K. M., "Beamwidth reduction of the binomial array for 5G communications," *2017 IEEE Region 10 Humanitarian Technology Conference (R10-HTC)*, 55–58, 2017.
35. Apostolov, P., B. Yurukov, and A. Stefanov, "Efficient three-element binomial array antenna," *2019 PhotonIcs & Electromagnetics Research Symposium — Spring (PIERS — Spring)*, 4127–4131, Rome, Italy, 2019.
36. Chopra, R., G. Kumar, and R. Lakhani, "Corner fed microstrip antenna array with reduced cross-polarization and sidelobe level," *2016 Asia-Pacific Microwave Conference (APMC)*, 1–4, 2016.
37. Computer simulation technology version (2018), Wellesley Hill MA. Available at: www.cst.com.
38. Rogers Corporation, available at: www.rogerscorp.com.